Optical design and performance comparison of various hyperspectral imagers based on Fery prisms

Yunfeng Nie,[a] Jingang Zhang,[b,c,*] Jing Wang,[d] Libin Xiang[b]
[a]Department of Applied Physics and Photonics, Vrije Universiteit Brussel, 1050 Ixelles, Brussels, Belgium
[b]Key Laboratory of Computational Optical Imaging Technology, Academy of Opto-Electronics of Chinese Academy of Sciences, 100094, Beijing, China
[c]University of Chinese Academy of Sciences, 100049, Beijing, China
[d]Département de physique, Université Laval, Québec, G1V 0A6, Canada

Abstract. The paraxial ray-tracing model of Fery prism is illustrated in this paper, and the three-order aberration coefficients are calculated. According to the solutions for minimal aberrations, four types of imaging spectrometers are designed based on Fery prism, accommodating for different requirements. The image quality is evaluated to ensure that MTFs are larger than 0.6 at Naquist frequencies, and the spectral resolutions are all higher than 5 nm. The advantages of these imaging spectrometers are analyzed by comparison of the volume, spectral resolution and field of view. The potential competence of Fery prism in hyperspectral imaging is indicated since the field of view and the volume have a direct proportional function. One typical system of these designs is manufactured and assembled afterwards to verify the simulation data.

Keywords: Hyperspectral imaging, Fery prism, optical design and spectral resolution.

***** Correspondence Author**,** E-mail: zhangjg@ucas.ac.cn

1 Introduction

Hyperspectral imaging systems enable simultaneous acquisition of cubic data which combines two-dimensional visual image with one-dimensional spectral information, closely related to the biochemical characteristics of specimen. This technique was originally applied to aviation and aerospace remote sensing [1-3], and then spread into fields as extensive as biomedical imaging, evaluation of fruit quality, food safety surveillance and so forth [4-6]. Recently, with the rapid development of photoelectric detection technology [7], spectral imaging has boomed into an even larger domain, from ultraviolet to far infrared spectrum [8, 9], from gigantic objects as forest and ocean to microorganism [10].

The most distinguished difference between a traditional camera and an imaging spectrometer is that the latter instrument contains at least one light-splitting element or method, which leads into fruitful categories of imaging spectrometer, such as the dispersive prism or grating type [11], the binary-optics type, the coded-aperture type, the Fourier Transform type [12] and the tunable

filter type [13]. From the perspective of light-splitting, two fundamental architectures are originally used to realize this kind of instrument, dispersive elements functioning in parallel and convergent (divergent) beams. The former system is much more mature with concise principle and low manufacture complexity; however, it's cumbersome and mass, not convenient for future usage. Fery prism was invented by C.Fery in 1911[14], describing as a prism with curved faces, which was then used in spectrophotometer[15] or monochromator [16]. After that, it was recently brought up into imaging spectrometer domain, with the success of CHRIS[17] and COMIS[18], utilizing in Offner configuration, where merits of compact structure, low mass as well as high image quality were achieved.

In this paper, we present the paraxial ray-tracing model and calculate the three-order aberration coefficients of Fery prism. According to the solutions for the equations, we design four different imaging spectrometers based on Fery prism, accommodating for different requirements. After that, we evaluate the image quality and analyze the advantages of different imaging spectrometers by comparing the volume, spectral resolution and field of view. One kind of these designs is manufactured and assembled afterwards to verify the simulation data.

2 Optical Model of Fery prism

Fery prism is different from the conventional flat prism. As shown in figure 1, Fery prism is a special optical element that has a circle aperture and two tilted spherical surfaces. If ABC represents for the contour of Fery prism with refractive index n, we can get an approximate thin prism $A'B'C'$ with flat surfaces. Thus, the dispersive resolution of the prism $A'B'C'$ can be roughly computed as follows:

$$D = \frac{\sin\alpha}{\cos i_1' \cos i_2'} \frac{dn}{d\lambda} \tag{1}$$

Where a is the vertex angle of the prism, $i_1^{'}$ and $i_2^{'}$ are the refraction angles of the front and back surfaces respectively. Generally, given a specific system where the incident angle is constant, refraction angles are determined by the index and incident angle. From equation (1), it can be inferred that adjusting the vertex angle and the material index can acquire suitable spectral resolution.

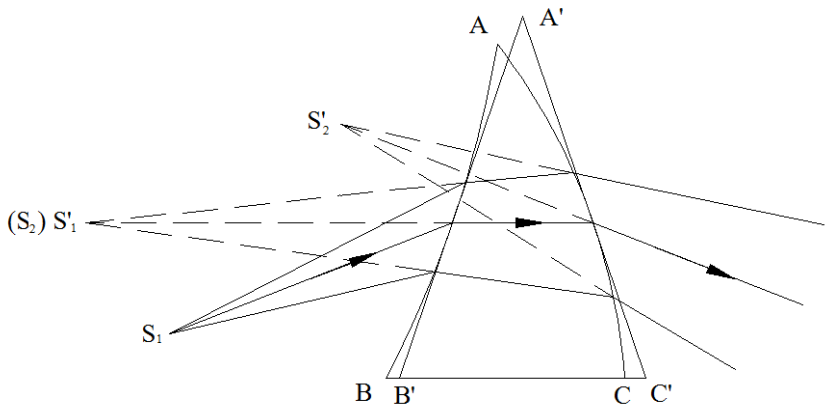

Fig.1. Paraxial ray-tracing model of Fery prism

Considering the imaging quality, paraxial ray-tracing method is used in calculating Seidel aberration coefficients of Fery prism so as to guide further optical design. In Fig.1, S_1 is a monochromatic object with distance l, and $S_1^{'}$ is the image of front surface as well as the virtual object of the back surface with distance l', and $S_2^{'}$ is the image of back surface. By applying Snell's law and angle identical equation, the image distance is determined by

$$l' = \frac{lRn'}{(n'-n)l + nR} \tag{2}$$

Where R is the radius of the computed spherical surface. By iteration, all parameters of every surface can be obtained. For simplification, assume the front and back surfaces have the same radii, so we can calculate the final image position using equation (2). With all the

parameters known, the primary aberration coefficients of single surface can be computed. Finally, the synthesized spherical, coma and astigmatic aberrations of single wavelength are formulated respectively as follows:

$$\begin{aligned}
&\sum A_1(\lambda) = 0 \\
&\sum A_2(\lambda) = \frac{1}{2}\frac{(n-1)a}{nl^2R^2}(R-l)\left[l-(n+1)R\right] \\
&\sum A_3(\lambda) = \frac{1}{2}\frac{(n-1)}{nlR}\left(na^2-2ai\right)\left[l-(n+1)R\right]
\end{aligned} \tag{3}$$

By solving the equations, we get two solutions for minimal aberration coefficients, $R = l$ and $R = l/(n+1)$, which are original architectures for optical design of Fery prismatic spectrometers. In other words, the object or image should be positioned in the distance $l = R$ or $l = (n+1)R$ from the Fery prism.

3 Optical design of distinct hyperspectral imagers

Based on the aberration theory above, we begin our design process as following steps. First of all, the reflective mirrors, which determine the main structure and foci, are built as a standard imaging system with moderate field of view and numerical aperture, for example, the single mirror and the Offner configuration. Secondly, the main parameters of Fery prism, such as radii and distances, are chosen to build the original architectures with corresponding imaging systems. There are mainly four styles qualified for the basic relations between radii and distance. The optical layouts are illuminated in Fig. 2, 3, 4 and 5, with the name of Single-Reflection, Two-Arm, and Middle-Arm and modified Two-Arm respectively.

As for the Single-Reflection and Two-Arm cases, either the object or the image is located on the aplanatic position ($l = (n+1)R$), where the convergence of a cone of rays is increased by a factor of index without the introduction of spherical aberration.

With regard to the Middle-Arm and modified Two-Arm cases, they both comply with the rule that the object or the image lies at the center of curvature ($l = R$), in which condition there is no spherical aberration introduced and the axial rays are not deviated.

After that, we adjust the vertex angle or material of Fery prism to obtain enough dispersion. The materials of high index are preferred since the vertex angle can be smaller, and a smaller deviation from optical axis introduces fewer aberrations. In the end, the variable parameters are set, and the Merit Function (MF) is defined to control aberrations, paraxial magnification, space, glass material, and spectral resolution and so on. Given that the imaging spectrometer always suits with an objective lens, the objective telecentric characteristic seems to be a priority when we do the design work.

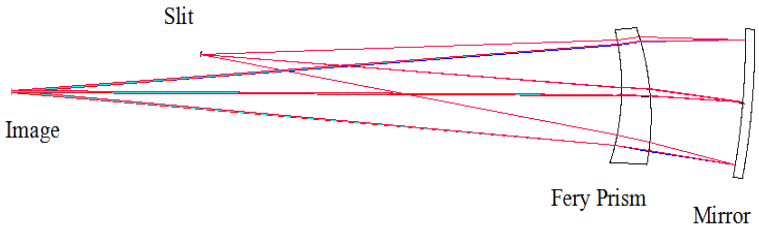

Fig.2. Optical schema of the Single-Reflection design

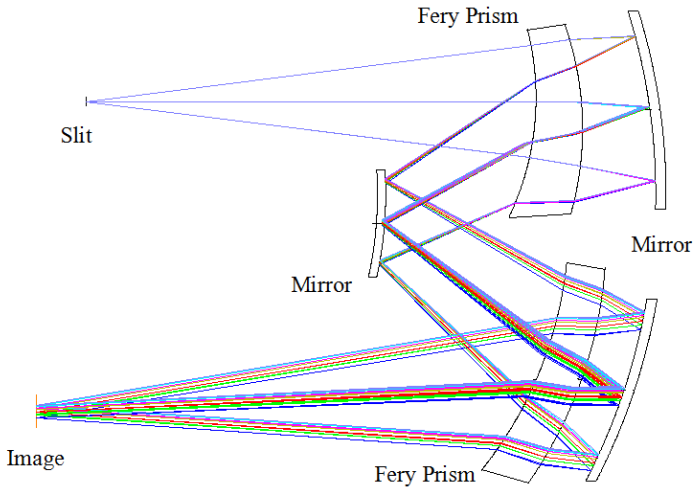

Fig.3. Optical schema of the Two-Arm design

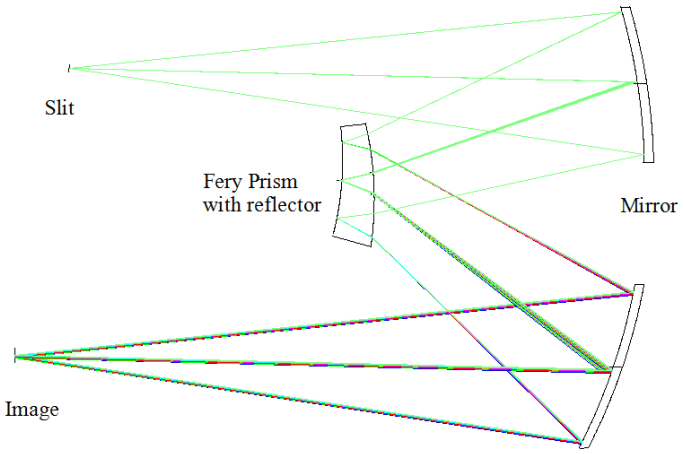

Fig.4. Optical schema of the Middle-Arm Design

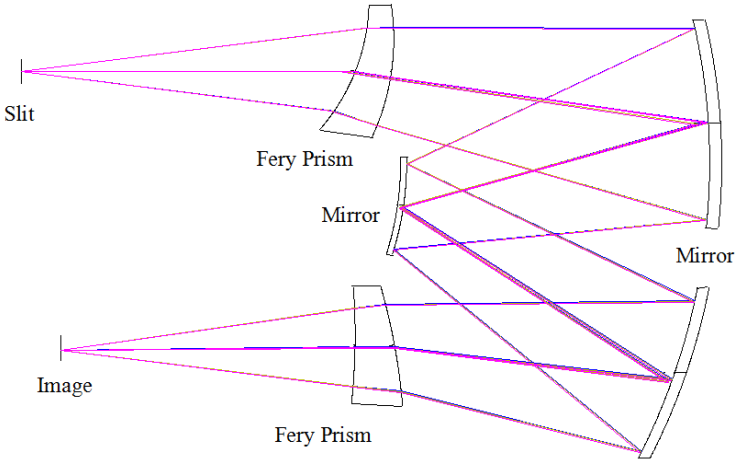

Fig.5. Optical schema of the modified Two-Arm design

Table1. The Parameters corresponding to Fig.2

Surface	Radius(mm)	Spacing(mm)	X Tilt(deg)	Glass
Object	Infinity	225	0	
1(5)	-102.408	15	-4	Quartz
2(4)	-115.287	50	-10.3	
Stop	-331.772	-325.24(from 5)	0.85	Mirror
Image	Infinity	0	0	

Table2. The Parameters corresponding to Fig.3

Surface	Radius(mm)	Thickness(mm)	Tilt/x(deg)	Glass
Object	Infinity	218	0	
1(5)	-134.229	22	0.78	Schott SF4
2(4)	-151.981	36	-4.96	

3	-301.34	-72.8(from 5)	0	Mirror
6	-187.37	72.8	0	Mirror
7(11)	-191.914	22	23.5	Schott SF4
8(10)	-208.55	36	19.5	
9	-301.762	-242(from 11)	0	Mirror
Image	Infinity	0	0	

Table 3. The Parameters corresponding to Fig.4

Surface	Radius(mm)	Thickness(mm)	Tilt/x(deg)	Glass
Object	Infinity	312.3	0	
1	-325.574	-158.7	-1.32	Mirror
2(4)	-178.734	-5	-21.7	Schott F2
3	-161.474	159(from 4)	0	Mirror
5	-325.574	-338.4	-1.32	Mirror
Image	Infinity	0	0	

Table 4. The Parameters corresponding to Fig.5

Surface	Radius(mm)	Thickness(mm)	Tilt/x(deg)	Glass
Object	Infinity	110	0	
1	-65.23	12	21.6	Schott F2
2	-76.115	105	8	
3	-205.312	-100	0	Mirror
4	-98.908	100	0	Mirror
5	-212.747	-105	0	Mirror
6	-203.362	-12	-11.8	Schott F2
7	-208.459	-96.875	-0.4	
Image	Infinity	0	0	

4 Performance evaluation and comparison

From the modulation transfer functions (MTFs) of the four designs, all of the values can approximate to the diffraction limit curve or be greater than 0.6 at their Nyquist frequencies, assuring the image quality requirements. As for spectral domain, we use the Monte-Carlo ray-tracing method to trace principal rays at different wavelengths and calculate the spectral resolution. As is known that prism dispersion is not linear, the spectral resolutions in Table 5 are numerical average values. We also trace different rays to get their two-dimensional positions at

different wavelengths in different fields. The statistics show that, both the frown and smile errors are corrected to an insignificant level as less than 0.2 pixels.

Table 5. Comparison among four types of Fery-prism imaging spectrometers

Parameters	Fig.2	Fig.3	Fig.4	Fig.5
Spectral resolution(nm)	5	1.7	4.3	3.4
Spectrum(nm)	450-1000	450-1000	450-1000	450-1000
Entrance slit(mm)	2	16	24	24
Numerical aperture	0.1	0.125	0.125	0.125
Sensor size(μm)	16	18	12	10
Paraxial magnification	1:1.4	1:1	1:1	1:1
Volume (cm^3)	39×7×7	30×22×10	34×25×10	21×13×9
Entrance Pupil	telecentric	telecentric	telecentric	telecentric
Vertex angle	6.3°	5.74°/4°	21.6°	13.6°/11.4°

As shown in Table 5, all the four systems can reach a moderate spectral resolution better than 5 nm. The spectrum can be flexible, since there are copious choices in prism materials, and the vertex angle can be altered.

The Single-Reflection design is compact and concise, merely containing two optical elements, the concept of which has already been realized in the PARISS instrument of Light Form Incorporation with wide application in nano-particle analysis and hyperspectral histopathology. Its field of view is a bit low, yet quite qualified for the hyperspectral microscopy.

By adding two concentric mirrors, we get the Middle-Arm design as in Fig.3 and Fig.4, which combine Offner relay configuration with Fery prism dispersion so as to achieve both larger field of view and higher resolution in spectral domain. By comparison to the Single-Reflection design, the Middle-Arm one is much more efficient, since it has a 12 times larger field and 1.3 times higher spectral resolution with the volume of only 5 times.

The Two-Arm system has its merit in greatly promoting the spectral resolution with four-time dispersions in two Fery prisms; however, it is still cumbersome in volume with a relatively small field of view limited by the degrading image quality and the increasing size of Fery prism.

With regard to the Two-Arm design, the modified Two-Arm system is merely the modified version by adjusting the position of Fery prism; however, it has a much more powerful competence in correcting aberrations and a smaller size. By sacrificing half of the spectral resolution, the field has increased by 50% and the volume has decreased by 63%.

After the detailed design and comparison above, the modified Two-Arm design is eventually chosen to build so as to verify our simulation. The Fery prism is much more difficult to manufacture than flat prism and lens for its multi-axes. It is overcome by a fine mechanical adjuster which can reach accuracy as high as 0.01^{o}. With precise fabrication and assembly, the system is doing well in the spectral and imaging tests. A front angle photograph of the assembled modified Two-Arm imaging spectrometer is shown in Fig. 6.

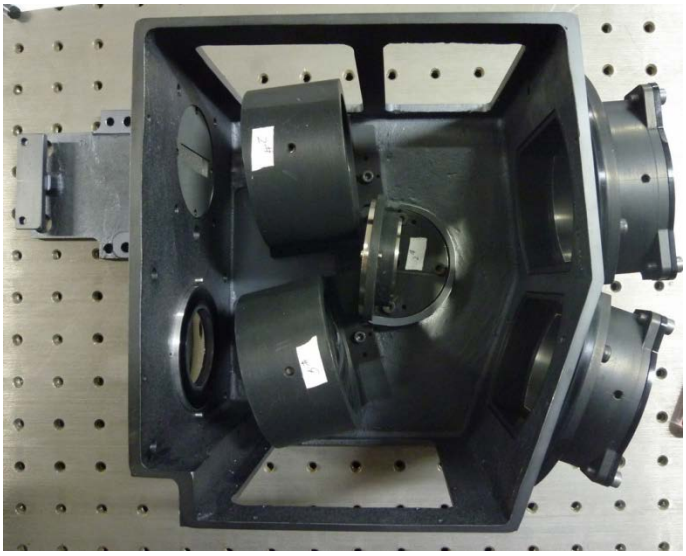

Fig.6. Photograph of the assembled modified Two-Arm imaging spectrometer

5 Conclusions

The paraxial aberration theory and dispersion approximation method of Fery prism are presented in this paper, which is the fundamental for designing hyperspectral imagers of this kind. Four different types of imaging spectrometers are modeled from two original architectures, suitable for different situations. The design results show that, imaging spectrometer based on Fery prism can reach a moderate spectral resolution from 1 nm to 10 nm, with a roughly estimated volume of 30×20×10 cubic centimeter. Considering the field of view is proportional to the volume, larger field can be obtained by scaling the design. The modified Two-Arm design has the best synthetic performance, from the perspectives of numerical aperture, field of view, image quality and volume, which can be a priority option for the spaceborne or airborne imaging spectrometer with large aperture and large field.

Acknowledgments

This work was supported by the Joint Foundation Program of the Chinese Academy of Sciences for equipment pre-feasibility study (No.6141A01011601), the National Natural Science Foundation of China (No. 61775219 and No. 61640422), and the Equipment Research Program of the Chinese Academy of Sciences (No. Y70X25A1HY and No. YJKYYQ20180039).

References

1. P. D. Hammer, F. P. Valero, D. L. Peterson, and W. H. Smith, Imaging interferometer for terrestrial remote sensing, *Proc. SPIE,* **1937,** 244-255 (1993).
2. V. V. Salomonson, W. L. Barnes, P. W. Maymon, H. E. Montgomery, and H. Ostrow, MODIS: advanced facility instrument for studies of the Earth as a system, *IEEE Transactions on Geoscience and Remote Sensing*, **27**(2), 145-153 (1989).

3. C. O. Davis, Spaceborne imaging spectrometer for environmental assessment of the coastal ocean, *Proc. SPIE*, **2817**, 224-230 (1996).
4. A. A. Gowen, C. P. O'Donnell, P. J. Cullen, G. Downey, and J. M. Frias, Hyperspectral imaging - an emerging process analytical tool for food quality and safety control, *Trends in Food Science & Technology*, **18**(12), 590-598 (2007).
5. J. M. Lerner, Imaging spectrometer fundamentals for researchers in the biosciences - A tutorial, *Cytometry Part A*, **69A** (8), 712-734 (2006).
6. C. Fischer and I. Kakoulli, Multispectral and hyperspectral imaging technologies in conservation: current research and potential applications, *Reviews in conservation*, **7**, 3-16 (2006).
7. Kuntao Ye and Xin Li, On the InGaAs-based Photodetection Circuit for Scanning Near-Infrared Signal in the Wavelength Range of 1.0-2.0μm, *JAOP*, **1**(1), (2018).
8. H. Tian, C. Tu, E. Marsch, J. He, and S. Kamio, The nascent fast solar wind observed by the EUV Imaging Spectrometer on board Hinode, *The Astrophysical Journal Letters*, 709, 88 (2010).
9. M. Kamruzzaman, G. ElMasry, D. Sun, and P. Allen, Non-destructive assessment of instrumental and sensory tenderness of lamb meat using NIR hyperspectral imaging, *Food Chemistry*, **141**(1), 389-396 (2013).
10. G.P. Asner, et al., Airborne laser-guided imaging spectroscopy to map forest trait diversity and guide conservation, *Science*, **385**, 385-389 (2017).
11. Nie, Y., et al., A Wide-Field Push-Broom Hyperspectral Imager Based on Curved Prism. *Spectroscopy and Spectral Analysis*, **32**(6), 1708-1711 (2012).
12. Zhang, C., X. Bin and B. Zhao. Static polarization interference imaging spectrometer (SPIIS). in *Applications of Photonic Technology 4*, pp. 1984-1997, Quebec City, Canada: SPIE (2000).
13. C. Fery, A prism with curved faces for spectrograph or spectroscope, *Astrophysical Journal*, **34**(1) 79-87(1911).
14. Romier, J., J. Selves and J. Gastellu-Etchegorry, Imaging spectrometer based on an acousto-optic tunable filter. *Review of Scientific Instruments*, **69**(8), 2859-2867(1998).

15. H. H. Cary and A. O. Beckman, A Quartz Photoelectric Spectrophotometer, *J. Opt. Soc. Amer.*, 31(11) (1941) 682-689.
16. R. Onaka, A vacuum Fery polarizing monochromator, *Japanese Journal of Applied Physics*, **20**(2), 417-421(1981).
17. M. A. Cutter, D. R. Lobb, T. L. Williams, and R. E. Renton, Integration and testing of the compact high-resolution imaging spectrometer (CHRIS), *Proc. SPIE*, **3753**, 180-191(1999).
18. J. Lee, T. Jang, H. Yang, and S. Rhee, Optical Design of a Compact Imaging Spectrometer for STSAT3, *J. Opt. Soc. Korea*, **12**(4), 262-268(2008).

Yunfeng Nie is a post-doctoral researcher at the department of applied physics and photonics of Vrije Universiteit Brussel. She graduated as BS.C. from University of Science and Technology of China (USTC) in the department of Precision Instrumentation and Precision Machinery in 2009, and obtained her MS.C. degree in optical engineering in 2012 from University of Chinese Academy of Sciences (CAS). During 2014 and 2017, she was offered the Marie Curie Scholar under European Commission's FP7 People Programme to do research in Vrije Universiteit Brussel (VUB) and obtained her PhD in Engineering Science. Her research interests include optical system design, hyperspectral imaging, freeform TMA telescopes, AR/VR head mounted display, high-resolution snapshot corneal imaging system, laser Raman spectrometer, etc. She is member of SPIE and OSA.

